

Supplemental Information

Polymer-coated TiO₂ nanoparticles bioaccumulate, immunoactivate and suppress pathogenic *Mycobacterium chelonae* clearance when intravenously injected into goldfish (*Carassius auratus L.*)

Van A. Ortega¹, David Boyle^{1,2}, Jordan W. Hodgkinson¹, Denina B. D. Simmons³, Miodrag Belosevic¹, James, L. Stafford¹, Greg, G. Goss^{1,4}

¹Department of Biological Sciences, University of Alberta, Edmonton, Canada

²School of Biological and Marine Sciences, University of Plymouth, Plymouth PL4 8AA, UK

³University of Ontario Institute of Technology, Faculty of Science, Oshawa, Ontario, L1H 7K4,
Canada

⁴University of Alberta-National Research Council of Canada Nanotechnology, Edmonton,
Alberta, Canada

***Corresponding author:** Van A. Ortega: Department of Biological Sciences, University of Alberta, Edmonton, Alberta, T6G 2E9, Canada. Tel: +1 780 492 1276; Fax: +1 780 492 9234;
Email: vortega@ualberta.ca

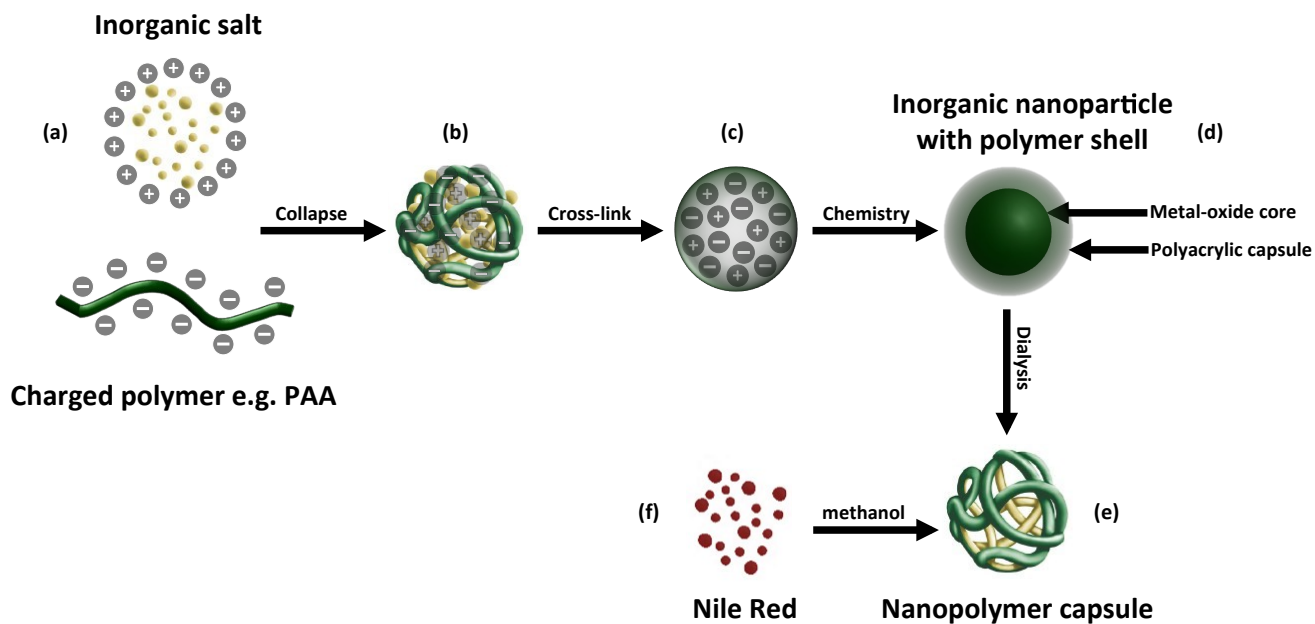
Principal Investigator: Greg G. Goss: Email: ggoss@ualberta.ca

Supplemental Information

1. PAA-NP Synthesis Protocol

The functionalized derivatives used in this study consisted of polyacrylic acid (PAA)-encapsulated metal oxide TiO_2 (rutile) that was manufactured by Vive Crop Protection Inc. (formerly Vive Nano Inc.) (Toronto, ON, Canada) and were kindly donated. The NP template was synthesized via interaction between oppositely charged PAA (120 kDa) polymer chains and inorganic counterions (i.e., inorganic Ti) (Figure 1a), resulting in condensed orb-like structures of negative charge that are less than 10 nm in size (Figure 1b).¹ These structures were then stabilized by cross-linking polymer chains either chemically or through ionizing radiation to maintain their integrity in suspension (Figure 1c). Finally, redox and precipitation reactions were used to convert the counterions encapsulated within the cross-linked coating to inorganic-oxide NPs, which are filtered through a membrane as a final purification step before being lyophilized for long-term storage (Figure 1d).^{2,3} A PAA-NP that contained the fluorescent dye, Nile Red, was also produced for this study and used as a photoluminescent NP to track uptake and translocation across tissues and cells. PAA-Nile Red NPs were produced in a similar manner as described above, where 0.2 g Nile red (excitation/emission wavelengths [Ex/Em] = 552/636 nm) were dispersed in methanol, causing an association between a dialysis-hollowed polymer NP capsule (Figure 1e) and the fluorescent dye, and then lyophilized (Figure 1f). The interaction of metal-oxides or dyes with the PAA polymer is defined by non-covalent interactions such as charge-charge interactions, hydrophobic interactions, polymer-chain interactions, van der Waals forces, or ionic interactions.³ Working suspensions were made from

lyophilized stocks and resuspended in sterile Cortland's saline. Lyophilized stocks were stored at 4°C and protected from light.



Supplemental Figure S1. Schematic diagram of polymer-coated NP synthesis, provided by Vive Crop Protection Inc. Interaction between oppositely charged polymer chains and counterions (a) results in condensed orb-like structures (b). These structures are then stabilized by cross-linking polymer chains either chemically or through ionizing radiation (c). Redox and precipitation reactions convert the counterions encapsulated within the cross-linked coating to inorganic NPs (d). Dispersing nile red dye in methanol causes an association between the polymer NPs and the fluorescent dye (e) to make the nile red-loaded nanocapsules (f).

2. PAA-NP Characterization

Manufacturer measurements for PAA-NP size, pH, metal purity, and percent metal composition are summarized in Supplemental Table S1. To determine trace metal content, lyophilized PAA-NPs were weighed, acidified with HNO₃ then measured using an Inductively Coupled Plasma Optical Emission Spectrometer (ICP-OES, Varian Vista-Pro CCD Simultaneous) equipped with an autosampler (Varian SPS 3). ICP-OES was coupled with Total Organic Carbon (TOC-VCPH Shimadzu analyzer) oxidative combustion-infrared analysis equipped with an autosampler (ASI-V) and solid sample module (SSM-5000A) (Supplemental Table S2). Results from Supplemental Tables S1 and S2 showed that sizes ranged between 3-9 nm and metal purity is above 98%. The pH of suspended PAA-TiO₂ was neutral, while the percent metal for PAA-TiO₂ was 46%, with the remaining likely contributed from the polymer and sodium stabilizer.⁴

In addition to manufacturer measurements, we have conducted extensive physico-chemical characterization of stock PAA-NPs. NP shape and primary particle size were confirmed with Transmission Electron Microscopy (TEM), using a JEOL-2010 (LaB6 filament) electron microscope with an accelerating voltage of 200 kV. Nanoparticles (10 µg/mL) in ultrapure water were drop-coated onto carbon coated copper grids (200 XXXµm) and air-dried at room temperature to remove any residual solvent prior to analysis. TEM imaging of NPs confirmed information from the manufacturer that the PAA-NP metal cores were 3-9 nm in size (Supplemental Figure S2).⁵

Dynamic Light Scattering (DLS; Zetasizer Nano Series, Malvern Instruments Inc.) was used to characterize PAA-TiO₂ size and aggregation by measuring hydrodynamic diameter,

polydispersity index, and zeta potential of PAA-test suspensions at a variety of concentrations (10, 50, 100, and 200 $\mu\text{g}/\text{mL}$) at 0 and 24 h. Results showed that in ultrapure water at time 0, mean hydrodynamic diameters of suspended particles were larger (approx. 40 nm) than primary metal core measurements indicating that some immediate aggregation occurred following suspension in ultrapure water (Supplemental Table S3). In general, the mean hydrodynamic size did not vary from 0 to 24 h for PAA-TiO₂ in ultrapure water or at each tested concentration. However, some distinct size populations were observed at 24 h, where there were discrete NP aggregate populations (Supplemental Figure S3).⁵ Polydispersity measurements showed PAA-TiO₂ to have mid-range PDI values (0.08-0.7) at all concentrations at both 0 and 24h, which indicates that some aggregation was likely occurring at all the tested concentrations (Supplemental Table S3). PAA-TiO₂ also had negative zeta potentials, indicating the NPs are negatively charged.⁵

Dissolution experiments have also been previously conducted to calculate the concentration of free metal ions present in NP stock suspensions and to determine the maximum concentration of metal ions released from the NPs over a 72 h dialysis period since nanotoxicity data is often misinterpreted as solely a NP effect when toxicity may be caused by free metal ions being released from the NPs. For both experiments, Slide-A-Lyzer dialysis cassettes (~1 nm; 2000 molecular weight cut-off (MWCO), Pierce) were injected in triplicate with either 0.5 mL of the 10 g/L NP stock suspension (PAA-TiO₂) and placed in a beaker of water. The concentration of free metal ions present in the stock suspensions and the concentration of free metal ions released over 72 hours were analyzed in collected water samples by Inductively Coupled Plasma Mass Spectroscopy (ICP-MS, Perkin Elmer, Elan 6000).

Results showed that primary metal ions, as trace contaminants, dialyzed from NP stocks over 30 minutes were $16.44 \pm 12.99 \mu\text{g/mL}$ (Ti^{4+}). As a percentage, this value converted to 1.07% (Ti^{4+}), which was considered negligible (Supplemental Table S4).⁴ Following the 30-min removal of free metal ions as trace contaminants from the stocks by dialysis, there was minor release of the metal ions from the NP metal core over a 72 h period (Supplemental Table S4). The relative amount of Ti metal released from the NP core remained consistently low, suggesting that the free metal in each stock suspension was removed by initial dialysis and that PAA-TiO₂ was stable and not dissolving overtime in our test media. The relative amount of free metal released from the NP core in PAA-TiO₂ (<1.5 $\mu\text{g/L}$) diluents over 72 h were nominal compared to the free metal ions released after 30 min of dialysis.⁴

The optical properties were measured for PAA-TiO₂ to characterize their intrinsic absorbance and fluorescence to account for possible interference with spectrophotometry assays that rely on absorbance or fluorescence as an endpoint measurement. PAA-TiO₂ was suspended in ultrapure water at 50 $\mu\text{g/mL}$ and loaded into a quartz cuvette. An absorbance spectrum from 190 – 820 nm (Hewlett Packard 8452A diode array spectrophotometer) and a fluorescence emission spectrum up to 1100 nm (excitation 250 nm, Cary Eclipse photoluminescence spectrometer) were then recorded. Absorbance occurred at nearly 1.0 a.u. for PAA-TiO₂ and did not display fluorescent properties (Supplemental Figure S4).⁶

Supplemental Table S1. Product lot number, particle size (nm), pH, total metal (%), and purity (%) of PAA-TiO₂.⁴

Nanoparticle	Lot Number	Size (nm)^a	pH	Total Metal (%)^b	Purity (%)^c
PAA-TiO ₂	PB 42	3-9	7.0	46	98

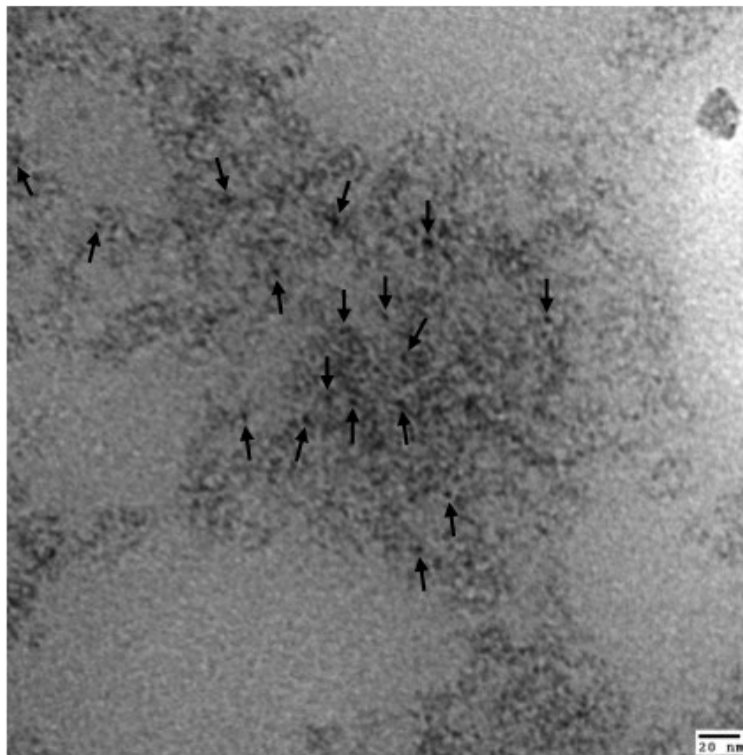
^aExclusive of PAA coating.

^bTotal metal, Ti

^cPurity is exclusive of Na⁺ stabilizer and PAA coating.

Supplemental Table S2. Trace metal (>0.1%), excluding Na⁺, of PAA-TiO₂ as analyzed by the manufacturer. Dashes indicate trace metal not present or below the ICP-MS detection limit.⁴

Trace metal (%)	PAA-TiO₂
Ag	0.5
Al	0.3
B	0.1
Ca	
Co	0.1
Cr	-
Ga	-
Gd	-
Ho	-
Ir	-
K	-
Li	-
Mg	-
P	-
Pr	-
Rb	-
Si	-
Zn	-



Supplemental Figure S2. Transmission electron micrographs (JEOL-2010 (LaB6 filament) electron microscope with an accelerating voltage of 200 kV) of Vive Crop Protection polyacrylic (PAA) functionalized nanoparticle PAA-TiO₂ showing sizes ranging between approximately 3 to 9 nm.⁵

Supplemental Table S3 Dynamic Light Scattering results showing mean hydrodynamic diameter (nm), zeta potential (mV) and polydispersity index of Vive Crop Protection polyacrylic (PAA) functionalized PAA-TiO₂, diluted to 10, 50, 100, and 200 µg/ml in ultrapure water at time 0 h and 24 h.⁵

Nanoparticle	DLS Parameter	Nanoparticle concentration (µg/mL)							
		10		50		100		200	
		0h	24h	0h	24h	0h	24h	0h	24h
PAA-TiO ₂	HD (nm)	29	28	32	37	31	30	31	28
	PDI	0.35	0.29	0.34	0.28	0.31	0.28	0.31	0.26
	ZP (mV)	-6	-8	-26	-22	-28	-27	-32	-28

Notes:

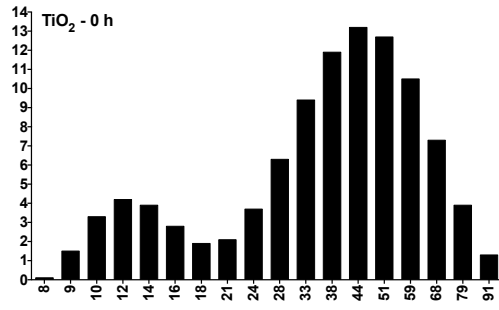
HD: Hydrodynamic diameter

PDI: Polydispersity Index

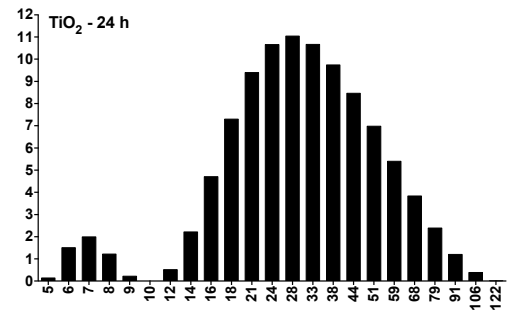
ZP: Zeta Potential

% Nanoparticle intensity

a.

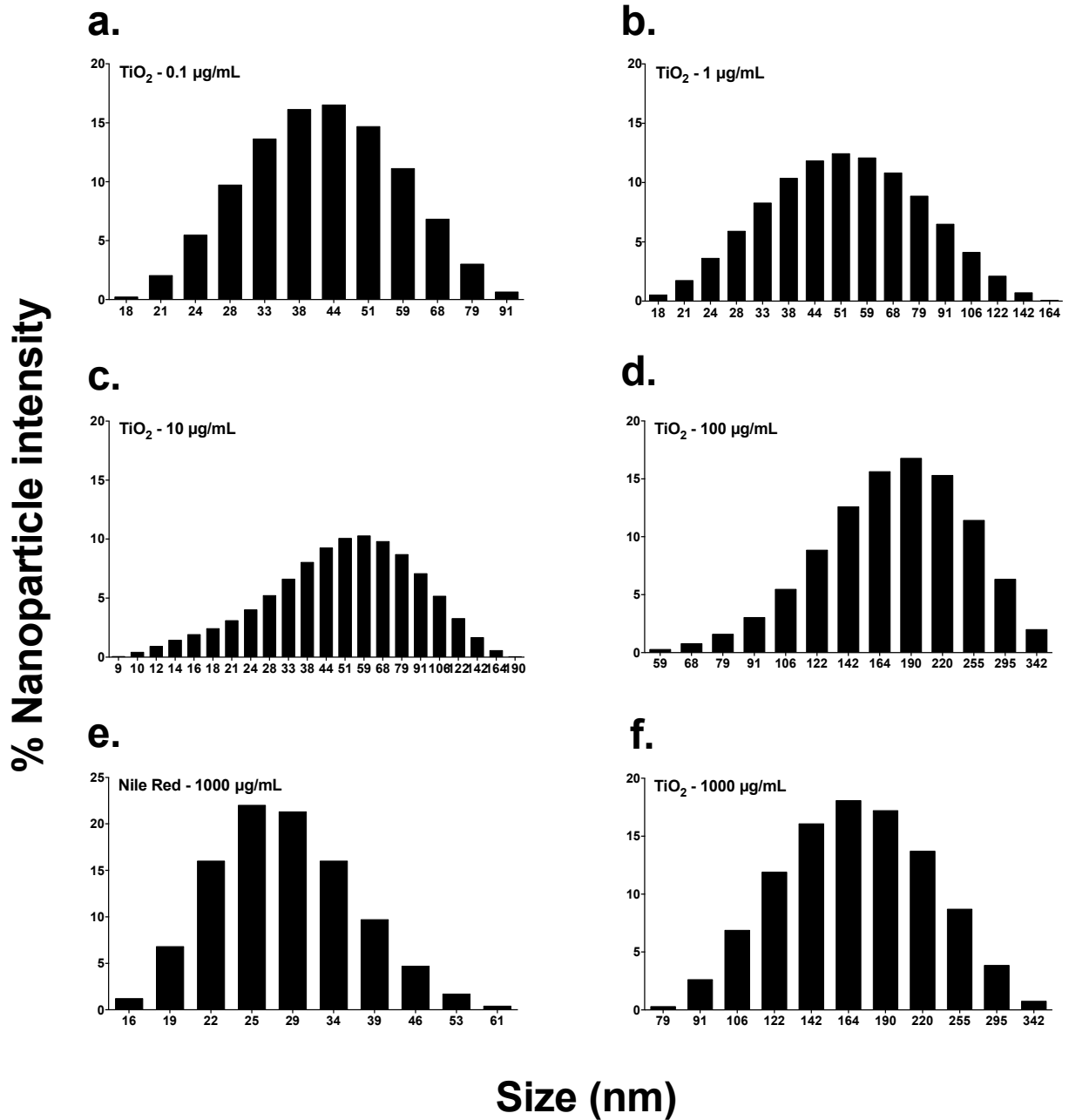


b.



Size (nm)

Supplemental Figure S3. Representative dynamic light scattering hydrodynamic size distributions (nm) of Vive Crop Protection polyacrylic (PAA) functionalized TiO_2 nanoparticles at 0 h (a) and 24 h (b), diluted to 200 $\mu\text{g}/\text{mL}$ in sterile ultrapure water.⁵



Supplemental Figure S4. Dynamic light scattering (DLS) mean hydrodynamic diameters (nm) of Vive Crop Protection polyacrylic acid (PAA)- TiO_2 NPs diluted to 0.1, 1, 10, 100, and 1000 $\mu\text{g/mL}$ and Nile Red NPs diluted to 1000 $\mu\text{g/mL}$ in Cortland's saline buffer at time 0 h.

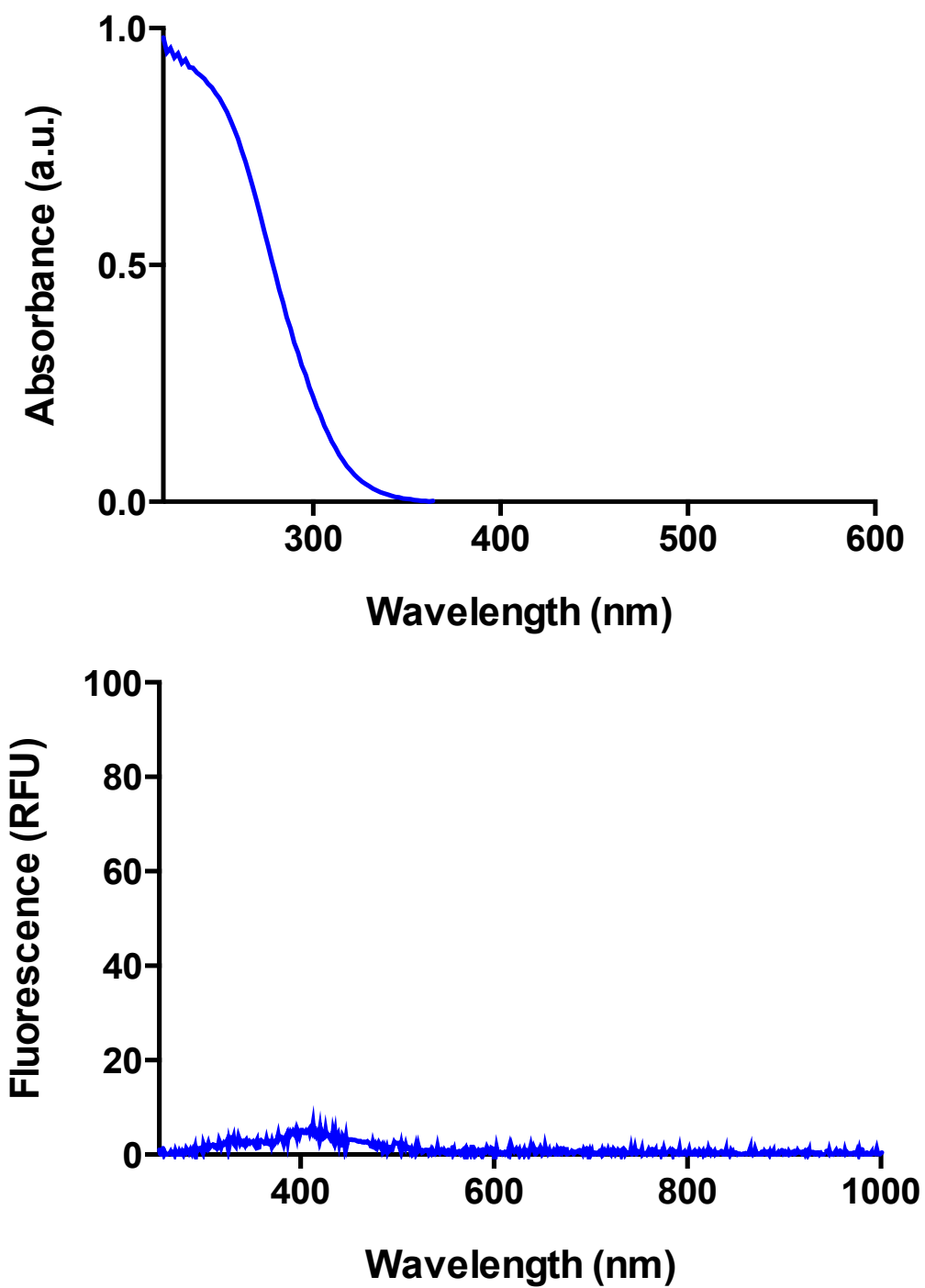
Supplemental Table S4. Primary particle size (nm), pH, metal purity (%), and percent free metal dialyzed following 30 min and 72 h of dialysis of Vive Crop Protection polyacrylic acid (PAA) functionalized TiO₂ suspended in ultrapure water.⁴

Nanoparticle	Primary particle size (nm)^a	pH	Purity^b (%)	Percent free metal dialyzed after 0.5 h (%)	Percent free metal dialyzed between 0.5 - 72 h (%)
PAA-TiO ₂	3-9	7.0	98.0	1.07	0.016

Notes:

^aExclusive of PAA coating

^bPurity is exclusive of Na⁺ stabilizer and PAA coating.



Supplemental Figure S5. Spectral measurements of optical characteristics of PAA-NPs Absorbance (a) and fluorescence (excited at 250 nm) (b) characteristics of PAA-TiO₂ at 50 $\mu\text{g}/\text{mL}$.⁶

3. PCR Primer Information

Supplemental Table S5. Forward (F) and reverse (R) primer sequences (5'-3') used for quantitative PCR measurements.

Primer name	Reference accession numbers	F / R	Primer sequence (5'-3')
EF-1 α ¹	AB056104.1	F	GTCAGCGCCTACATCAAGAA
		R	CCCTTGAACCAGCCCATATT
IL-10	HQ259106.1	F	GCTTCTACTTGGACACCATTCT
		R	ATCCCGCTTGAGATCCTTAAAT
TNF α	EU069817.1	F	CCTAGACTGGAAACAGAACCAG
		R	GGAAAGACACCTGACTGTAGAC
IL-1 β 1	AJ419848.1	F	GGAGAATGTGATCGAAGGTACAG
		R	GCTGGTGCTTCCAGCTTTA
GCSFR	JF922012.1	F	GCTGGGCTCTGTCTCTAATTC
		R	AGTCTCCACTCTAGCACGTATC

Notes: ¹Endogenous control

Supplemental Table S6. Forward (F) and reverse (R) primer sequences (5'-3') used for PCR measurements of *Mycobacterium*.

Primer name	F / R	Primer sequence (5'-3')
Mycobacterium	F	AGAGTTTGATCCTGGCTCAG
	R	CATCCACACCGCWAAAG

REFERENCES

1. Vive Crop Protection, Vive Crop Protection: Specializing in formulation and delivery of active ingredients., <http://www.vivecrop.com/technology.html>, (accessed 5 February 2013).
2. Goh, C.M., Dinglasan, J.A., Goh, J.B., Loo, R., Veletanlic, E., 2009. Composite nanoparticles, nanoparticles and methods for producing same. 7534490.
3. Li, F., Pham, H., Anderson, D.J., 2011. Methods to produce polymer nanoparticles and formulations of active ingredients. US8084397 B2.
4. L. C. Felix, V. A. Ortega, J. D. Ede and G. G. Goss, Physicochemical Characteristics of Polymer-Coated Metal-Oxide Nanoparticles and their Toxicological Effects on Zebrafish (*Danio rerio*) Development, *Environ. Sci. Technol.*, 2013, **47**, 6589–6596.
5. V. A. Ortega, B. A. Katzenback, J. L. Stafford, M. Belosevic and G. G. Goss, Effects of polymer-coated metal oxide nanoparticles on goldfish (*Carassius auratus L.*) neutrophil viability and function, *Nanotoxicology*, 2015, **9**, 23–33.
6. V. A. Ortega, J. D. Ede, D. Boyle, J. L. Stafford and G. G. Goss, Polymer-Coated Metal-Oxide Nanoparticles Inhibit IgE Receptor Binding, Cellular Signaling, and Degranulation in a Mast Cell-like Cell Line, *Adv. Sci. Weinh. Baden-Wurtt. Ger.*, 2015, **2**, 1500104.